Global Change Biology (2009) **15**, 116–131, doi: 10.1111/j.1365-2486.2008.01705.x

Uncertainties in the response of a forest landscape to global climatic change

CHONGGANG XU*, GEORGE Z. GERTNER* and ROBERT M. SCHELLER†
Department of Natural Resources and Environmental Sciences, University of Illinois, 1102 South Goodwin Avenue, Urbana, IL 61801, USA, †Conservation Biology Institute, 136 SW Washington, Suite 202, Corvallis, OR 97333, USA

Abstract

Many studies have been conducted to quantify the possible ecosystem/landscape response to the anticipated global warming. However, there is a large amount of uncertainty in the future climate predictions used for these studies. Specifically, the climate predictions can be very different based on a variety of global climate models and alternative greenhouse emission scenarios. In this study, we coupled a forest landscape model, LANDIS-II, and a forest process model, PnET-II, to examine the uncertainty (that results from the uncertainty in the future climate predictions) in the forest-type composition prediction for a transitional forest landscape [the Boundary Water Canoe Area]. Using an improved global-sensitivity analysis technique [Fourier amplitude sensitivity test], we also quantified the amount of uncertainty in the forest-type composition prediction contributed by different climate variables including temperature, CO_2, precipitation and photosynthetic active radiation (PAR). The forest landscape response was simulated for the period 2000–2400 AD based on the differential responses of 13 tree species under an ensemble of 27 possible climate prediction profiles (monthly time series of climate variables). Our simulations indicate that the uncertainty in the forest-type composition becomes very high after 2200 AD, which is close to the time when the current forests are largely removed by windthrow disturbances and natural mortality. The most important source of uncertainty in the forest-type composition prediction is from the uncertainty in temperature predictions. The second most important source is PAR, the third is CO_2 and the least important is precipitation. Our results also show that if the optimum photosynthetic temperature rises due to CO_2 enrichment, the forest landscape response to climatic change measured by forest-type composition may be substantially reduced.

Keywords: Boundary Water Canoe Area, forest landscape, global climatic change, LANDIS-II, PnET-II, sensitivity, uncertainty

Received 20 August 2007; revised version received 15 June 2008 and accepted 11 July 2008

Introduction

We are in a time of unprecedented climatic warmth during the past 1200 years due to anthropogenic disturbances (Osborn & Briffa, 2006). According to the Intergovernmental Panel on Climate Change (IPCC), the global mean surface temperature will continue to increase by 1.4–5.8 °C over the next 100 years, mainly due to the CO_2 enrichment by fossil fuel use (IPCC, 2001). The corresponding precipitation and photosynthetic active radiation (PAR) may also increase or decrease depending on a specific spatial location (IPCC, 2001). Forest ecosystems are one of the world's most important ecosystems that may be substantially affected by this global climatic change (Dale *et al*., 2001). Climatic change may affect tree species abundance, distribution, forest community characteristics (e.g. species richness and diversity) and biome distributions (Hansen *et al*., 2001). Forest ecosystems near the southern and northern ranges of their distributions are expected to have the strongest responses to climatic change (Pastor & Post, 1988; He *et al*., 2005). Under global climatic change, a temperature increase in the northern hemisphere could benefit southern species by providing their optimal growing temperatures and could be detrimental to northern species by putting

Correspondence: George Z. Gertner, e-mail: gertner@vivc.edu

them in a state of supra-optimal growing temperatures (Xu *et al*., 2007). Precipitation may affect soil water availability and thus species performance in future climatic conditions (Pastor & Post, 1988; Koerner *et al*., 2005; Suttle *et al*., 2007). PAR is the energy source for photosynthesis and may vary under global climatic change depending on predicted cloud cover and albedo. Simultaneously, CO_2 enrichment can stimulate the photosynthesis of tree species and restrict photorespiration (Drake *et al*., 1997; Long *et al*., 2004; Korner, 2006). Furthermore, CO_2 enrichment can reduce stomatal conductance (Saxe *et al*., 1998; Medlyn *et al*., 2001). In addition to individual climate variables, the interactions among them may also play a very important role. For example, the stomatal conductance reduction caused by CO_2 enrichment may increase the water use efficiency of trees and relieve the soil water availability stress caused by the increase in temperature.

There have been many studies focusing on the forest ecosystem and landscape response to climatic change using gap models (Pastor & Post, 1988; Urban *et al*., 1993; Sykes & Prentice, 1995; Keane *et al*., 2001), spatially dynamic forest landscape models (He *et al*., 1999, 2002; Scheller & Mladenoff, 2005), statistical analysis of current species distributions against climate variables by regression tree analysis (Iverson & Prasad, 1998; Iverson *et al*., 2004) and response surface analysis (Flannigan & Woodward, 1994; Shafer *et al*., 2001). However, there is a large amount of uncertainty in the future climate (temperature, precipitation, CO_2 and PAR) predictions that are used for these studies. Specifically, the climate predictions can be very different based on a variety of global climate models and alternative greenhouse emission scenarios. The amount of CO_2 emissions in the future depends much on the intensity of fossil fuel use and new technology developments. The uncertainty in CO_2 emissions is addressed by IPCC using different greenhouse gas emission scenarios (Leggett *et al*., 1992; Nakicenovic & Swart, 2000; IPCC, 2001). For a specific spatial location, the temperature, precipitation and solar radiation prediction may be very different among alternative greenhouse gas emission scenarios. Furthermore, the predictions can be different among a variety of model simulations based on the same greenhouse gas emission scenario (Mahlman, 1997; Weaver & Zwiers, 2000; Kerr, 2001; Schwartz *et al*., 2002). In view of the large amount of uncertainty in climatic change predictions, it is therefore important that we evaluate the uncertainty in forest landscape response to climatic change, because the ecosystem response may be significantly different under different climate change predictions (Suttle *et al*., 2007).

The uncertainty quantification process generally includes uncertainty analysis and sensitivity analysis (Saltelli *et al*., 2000). Uncertainty analysis evaluates the amount of uncertainty in the model output, while sensitivity analysis evaluates how the uncertainty in the model output can be apportioned to different model parameters (Saltelli *et al*., 2000; Crosetto & Tarantola, 2001). For the uncertainty analysis of community and ecosystem response to climatic change, we first need an ecological model that links climate variables to forest landscape response. Based on such a model, we can use uncertainty and sensitivity analysis techniques to quantify the uncertainty in the response of forest landscape, and the corresponding contribution by different climate variables. However, the uncertainty and sensitivity analysis may not be simple, because the forest landscape response is generally a nonlinear complex process and climate variables are generally not independent (e.g. temperature may be correlated with CO_2). Using two recent important extensions to the Fourier amplitude sensitivity testing (FAST) (Tarantola *et al*., 2006; Xu & Gertner, 2007, 2008), a popular uncertainty and sensitivity analysis technique originally developed by Cukier *et al*. (1978), we are able to conduct the uncertainty and sensitivity analysis of community and ecosystem response to climatic change with complex nonlinear process and dependent model inputs.

Although the uncertainty in global climatic change has been acknowledged in earlier studies (Mahlman, 1997; Weaver & Zwiers, 2000), there are only a few studies attempting to quantify the uncertainty in species/ecosystem/landscape response as a result of uncertainty in climatic change prediction. Iverson & Prasad (2002) examined the potential redistribution of tree species habitat under five climate change scenarios in the eastern USA based on regression tree analysis. Thuiller (2004) quantified the uncertainty in species range shift and the contribution by climate change scenarios, niche models and a cut-off method (to derive probability values from models into presence–absence data). However, no studies have been conducted to specifically quantify the contribution of different climate variables to the uncertainty in forest landscape response, which is important for our understanding and prediction of future landscape response to climatic change.

In this study, we coupled a spatially dynamic forest landscape model, LANDIS-II, and a forest ecosystem process model, PnET-II, to examine the uncertainty in the forest-type composition prediction for a transitional forest landscape as a result of uncertainty in the climatic change prediction. In the simulation of forest landscape response to climatic change, we considered the interactions among climate variables and the differential

responses among different species. Using the FAST technique, we quantified the amount of uncertainty in the forest-type composition prediction contributed by different climate variables including temperature, precipitation, CO_2 and PAR.

Study area

Our study area (about 195 000 ha) is part of the Boundary Waters Canoe Area (BWCA) in northern Minnesota, USA (Fig. 1). BWCA has a cold temperate continental climate (Heinselman, 1973). The area is dominated with numerous lakes of difference sizes, accounting for about 17% of the study area. Soils are generally thin due to glacial scouring, although some till, outwash and lacustrine deposits exist. The main soils are inceptisols, entisols and histosols (Moser *et al*., 2007). Soil type and depth to bedrock are highly heterogeneous at fine spatial scales (Heinselman, 1973). Topography in the study area is relatively homogenous with local difference in elevation ranging from 30 to 150 m (Heinselman, 1973; Baker, 1989).

BWCA forests are transitional between boreal forests and Great Lakes north temperate forests. Because of high fire frequency, the BWCA forests were historically dominated by even-aged stands of two fire-adaptive species: jack pine (*Pinus banksiana*) and quaking aspen (*Populus tremuloides*) (Scheller *et al*., 2005). Because of fire suppression since the 1910s (Baker, 1992; Frelich & Reich, 1995), the shade-intolerant and early-to-midsuccessional species are being replaced by shade-tolerant species including white spruce (*Picea glauca*), black spruce (*Picea mariana*), balsam fir (*Abies balsamea*) and white cedar (*Thuja occidentalis*) (Scheller *et al*., 2005).

Almost all of the presettlement flora and fauna native to the area are currently present in the BWCA forests (Heinselman, 1973; Scheller *et al*., 2005). The main tree species include red pine (*Pinus resinosa*), jack pine, white pine (*Pinus strobus*), black spruce, white spruce, balsam fir, white cedar and quaking aspen (Heinselman, 1973; Baker, 1989). Other species including red maple (*Acer rubrum*), white ash (*Fraxinus americana*), sugar maple (*Acer saccharum*), paper birch (*Betula papyrifera*) and balsam poplar (*Populus balsamifera*) are also present (Heinselman, 1973; Scheller *et al*., 2005).

Methodology

We coupled a spatially dynamic forest landscape model, LANDIS-II (Scheller *et al*., 2007), with a forest ecosystem process model, PnET-II (Aber *et al*., 1995; Ollinger *et al*., 2002), to simulate the forest landscape response (measured by the forest-type composition) to future climatic change. The LANDIS-II model simulates the forest-type composition response to future climatic change by modifying the species' competitive and colonization ability. In the LANDIS-II model, the species' competitive ability under future climate may change through modification of the growth rate determined by the aboveground net primary production (ANPP). The colonization ability may change through the modification of the species establishment probability (SEP), which defines the probability of seedling establishment (assumes no competition from other species) under a specific climate. The PnET-II model is used to provide the estimate of ANPP and SEP under future climates (Fig. 2). The simulated ANPP and SEP in PnET-II are driven by climate variables including temperature, precipitation, CO_2 and PAR.

There may be different sources of uncertainty in the forest-type composition prediction including uncertainty in model inputs [vector inputs for the model including spatial or profile (time series) data, e.g.,

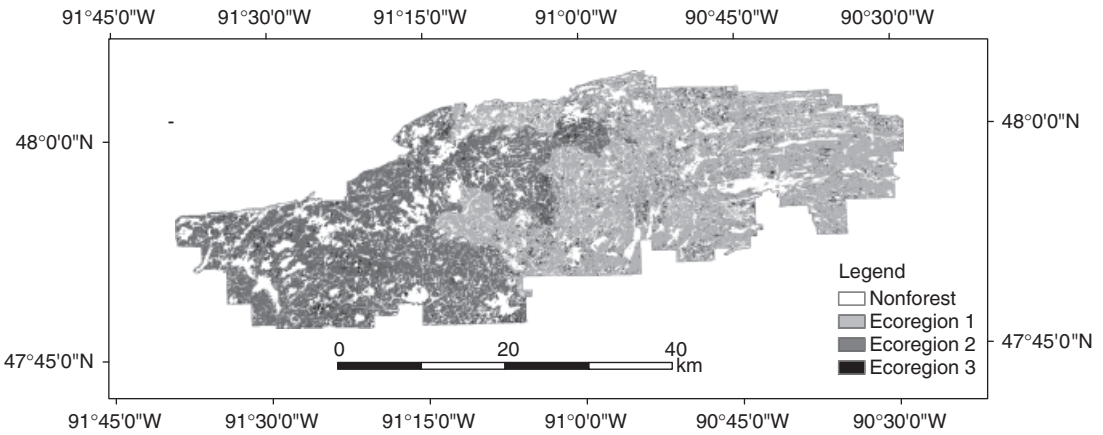

Fig. 1 Study area within the Boundary Waters Canoe Area Wilderness, Minnesota, USA.

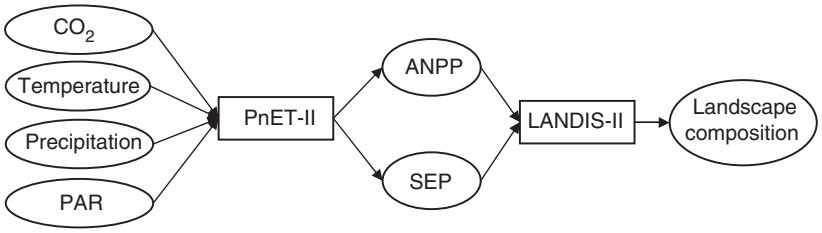

Fig. 2 Flow diagram of model coupling. The ovals represent input/output variables for a certain model. The rectangles represent models. ANPP, above ground primary production; SEP, species establishment probability.

spatial map of species composition or time series of monthly temperature input], model parameters [scalar variables for the model (e.g. the soil water holding capacity for the study area)] and model structure. In this study, our main focus was the uncertainty in the model inputs of temperature, precipitation, CO_2 and PAR. We did not take into account other potential sources of uncertainty, which may be very important for the forest landscape change prediction (Cramer *et al*., 2001; Xu *et al*., 2004). In order to determine the amount of the uncertainty in the future climate predictions, we selected 27 climate prediction profiles (monthly time series of climate variables) from the major global climate models under seven major greenhouse gas emission scenarios.

The FAST analysis based on Xu & Gertner (2008) was employed to assess the uncertainty in forest-type composition prediction during the period 2000–2400 AD.

PnET-II model

The PnET-II model was used to provide the ANPP and SEP inputs of LANDIS-II for each species (Scheller & Mladenoff, 2005). The model is a process-based model for carbon and water dynamics in forest ecosystems (Aber & Federer, 1992; Aber *et al*., 1995; Ollinger *et al*., 2002). The core relationship in the model is a linear response of maximum net photosynthetic rate to foliar N concentration. The original version of PnET-II does not include the effect of increased CO_2 on the forest production. In this study, we used the 5.1 version of PnET-II which includes an algorithm for the increased CO_2 effect on the photosynthesis and water use efficiency (Ollinger *et al*., 2002). The PnET-II model simulates the effect of climatic change on forest photosynthesis by applying an adjusting factor of light (dependent on input of PAR), temperature (dependent on the deviance of current temperature from the optimum photosynthetic temperature for specific species), water availability (dependent on input of precipitation), water vapor deficit and CO_2. The CO_2 enrichment may also increase the water use efficiency by reducing the stomatal conductance (Saxe *et al*., 1998; Medlyn *et al*., 2001). In the PnET-II model, the effect of CO_2 enrichment on the water use efficiency is simulated by using an adjusting factor related to stomatal conductance determined by the ratio of CO_2 flux across the leaf surface and the CO_2 concentration gradient from ambient air to the leaf interior (Ollinger *et al*., 2002). Because the stomatal conductance reduction due to CO_2 enrichment is much stronger in deciduous trees than that in coniferous trees (Medlyn *et al*., 2001), we only simulated the effect of CO_2 enrichment on the water use efficiency for deciduous trees.

The PnET-II model did not specifically calculate SEP. The seedling establishment is related to the seed germination, seedling growth and mortality, which may depend on the light levels, temperature and soil moisture (He *et al*., 1999; Castro *et al*., 2004). In this study, we calculated the SEP by the product of the environmental adjusting factors of light, water availability and vapor pressure deficit for photosynthesis (calculated in PnET-II), and another adjusting factor of growing degree days based on the deviance of actual growing degree days from the optimum growing degree days for a specific species, which are commonly used to represent the overall effect of temperature on tree growth (Botkin *et al*., 1972; Pastor & Post, 1985).

The species-specific parameters for PnET-II include foliar nitrogen content, optimal photosynthetic temperature, maximum leaf mass area and leaf retention time (Table 1). The optimum photosynthetic temperature is calculated based on the median of mean July temperature for species distributions in North America (Xu *et al*., 2007). The other parameters (including foliar N content, maximum leaf mass area and leaf retention time) are from Scheller & Mladenoff (2005).

LANDIS-II model

The LANDIS-II model is a spatially dynamic forest landscape model of disturbance, succession and management (Scheller & Mladenoff, 2004; Scheller *et al*., 2007). In LANDIS-II, the forest landscape is first divided

Table 1 Main species attribute parameters

Species	LNG	MTR	ST	ED	MD	VP	MAXVP	GGDMin	GDDMax	POT	FNC	MLMA	LRY
Aspen	160	25	1	200	5000	0.9	90	743	2900	20.0	2.5	83	1.0
Paper birch	230	30	2	200	5000	0.5	70	484	2036	18.8	2.3	100	1.0
Balsam poplar	150	25	1	200	5000	0.4	150	555	2491	17.7	2.5	80	1.0
Red maple	150	10	3	100	200	0.5	150	1260	6600	25.1	2.4	75	1.0
Sugar maple	300	40	5	100	200	0.1	240	1222	3100	25.0	2.5	85	1.0
White ash	200	30	4	70	140	0.1	70	1298	5993	25.5	2.1	76	1.0
Red pine	300	40	2	12	275	0	0	1100	2035	21.5	1.5	250	2.3
White pine	350	40	3	100	250	0	0	1100	3165	22.5	2.2	175	3.0
Jack pine	200	15	1	20	40	0	0	830	2216	19.9	2.3	244	1.6
White spruce	250	40	4	30	200	0	0	280	1911	17.8	1.5	286	4.0
Black spruce	200	20	3	80	300	0	0	247	1911	17.7	1.5	286	4.0
Balsam fir	150	25	5	30	160	0	0	560	2386	19.6	1.6	204	4.0
White cedar	300	35	4	45	60	0	0	1000	2188	21.0	1.3	222	2.0

LNG, longevity (years); MTR, age of maturity (years); ST, shade tolerance (one least tolerant and five most tolerant); ED, effective seeding distance (m); MD, maximum seeding distance (m); VP, vegetative reproduction probability; MAXVP, maximum age of vegetative reproduction (years); GGDMin, minimum growing degree days; GDDMax, maximum grow degree days; POT, optimum temperature for photosynthesis (°C); FNC, foliage nitrogen content (%); MLMA, maximum leaf mass area ($g\,m^{-2}$); LRY, leaf retention years (years).

Data for POT are from Xu *et al*. (2007); data for GGDMin and GDDMax are from Pastor & Post (1985) and other data are from Scheller *et al*. (2005).

into environmentally homogenous ecoregions, which have the same soil and climate conditions. Each ecoregion is composed of different cells/sites. LANDIS-II model tracks species and age cohort information at the site level. Two major types of ecological processes are simulated in LANDIS-II: nonspatial processes at the site level (e.g. species establishment and succession) and spatially interactive processes across different sites (e.g. seed dispersal, fire and harvesting). With LANDIS-II, the forest landscape change is driven by species life history attributes; species establishment probabilities; the biomass growth rate determined by the maximum ANPP disturbances; and spatial heterogeneity.

The main inputs for LANDIS-II include spatial inputs (an initial species and age cohort map and an ecoregion map) and nonspatial inputs (species life history attributes, ANPP, SEP and disturbance regimes). The initial species and age cohort map was derived from thematic image interpretation maps and forest stand age maps (Scheller *et al*., 2005). For the ecoregion map, the study area was divided into three ecoregions (Fig. 1). Ecoregion 1 and Ecoregion 2 were derived from the State Soil Geographic Data Base (STATSGO, 1994; Scheller *et al*., 2005), which mainly differ in the soil water holding capacity (average soil water holding capacity was 6.67 cm for Ecoregion 1 and 10.02 cm for Ecoregion 2). Ecoregion 3 was limited to areas designated as pure black spruce forests. Species life history attributes are based on Scheller *et al*. (2005) (Table 1). The maximum age of species ranges from 150 to 300 years. As already mentioned, due to fire suppression, fire rotation periods are very long (>1000 years) relative to presettlement conditions (Frelich & Reich, 1995). In this study, we simulated the windthrow disturbances with a rotation period of 500 years for all scenarios (Scheller *et al*., 2005).

Climatic change data

Future climatic change inputs for PnET-II were derived from the IPCC Third and Fourth Assessment Reports, and the Phase-II Vegetation-Ecosystem Modeling and Analysis Project (VEMAP) report (Kittel *et al*., 2000). Because the global climatic change predictions were based on coarse grid data (0.5° latitude/longitude grid for VEMAP and >1° latitude/longitude grid for IPCC projects), we used a bilinear interpolation to extract the values of climate variables for the centroid of our study area. In view that the data may have bias due to the coarse resolution, the climate variable predictions were calibrated using historic data from the DAYMET US Data Center (http://www.daymet.org/) (Thornton *et al*., 1997) during the period 1980–2000 AD. Namely, we first calculated the monthly bias of the prediction data from the historical data averaged across the period 1980–2000 AD. If the monthly bias was positive (i.e. the predicted monthly value was larger than the historical data during the period 1980–2000 AD), then it was subtracted from the predicted monthly values. Otherwise, it was added to the predicted monthly values. All the climate predictions for the period 2000–2099 AD had

an annual mean temperature bias $< 2.5\,^{\circ}C$, except for predictions from the Japanese National Institute for Environmental Studies used for the IPCC Fourth Assessment Report. For this institute, annual mean temperature bias was $> 3.5\,^{\circ}C$ for all scenarios. Because the high bias may indicate that this global climate model was not well parameterized for our study area, we did not incorporate it in our study.

In addition, necessary inputs for PnET-II required predictions of monthly maximum and minimum temperature, precipitation, CO_2 concentration and total incident solar radiation. According to the above criteria, there were 27 climate prediction profiles (monthly time series data) for the period 2000–2099 AD. Because the 27 climate prediction profiles encompassed the major global climate models under seven major greenhouse gas emission scenarios (A1T, A1FI, A2, B1, B2, A1B and IS92a) (Table 2), they may have well captured the uncertainty in climatic change prediction, although not all available climatic change predictions were included. For definitions of these different emission scenarios, refer to Leggett *et al*. (1992), Nakicenovic & Swart (2000) and IPCC (2001).

For the 27 selected climate prediction profiles, the mean CO_2 concentration ranged from 546.80 (scenario: B1) to 923.25 ppm (scenario: A1FI) in 2099 AD (Fig. 3a). There was roughly 2–8 °C annual mean temperature increase during the period 2000–2099 AD (Fig. 3b) and a relatively slight increase in the annual precipitation as compared with the interannual variability within the predictions (Fig. 3c). The climate models indicated a slight decrease in mean PAR during the period 2000–2099 AD, except for emission scenarios A1FI and A1T.

Uncertainty and sensitivity analysis

We used the FAST technique to assess the uncertainty in the forest-type composition prediction as a result of uncertainty in the climate predictions during the period 2000–2400 AD. The FAST analysis generally deals with uncertainty in model parameters, which are usually scalar variables. For the general FAST analysis, the uncertainty in the model output is represented by the variance of model output values and the uncertainties in the parameters are represented by specified probability distributions. In order to determine the amount of uncertainty in model output contributed by different model parameters, the FAST uses a periodic sampling function (an arcsine function which has a distinct integer frequency or characteristic frequency for a specific parameter) to sample values from the parameter probability distribution. Then, the model is run with the sampled parameter values to get the model output. Because the model output may also become periodic due to the periodically sampled parameter values, a Fourier transformation can be applied to the model output to decompose the variance of the model output into variances over the integer frequencies (Cukier *et al*., 1978). Finally, the amount of variance in the model output contributed by a specific parameter can be determined based on the characteristic frequency. The contribution of a specific model parameter to the uncertainty in model output (sensitivity index) is calculated as the ratio of amount of variance contributed by the parameter to the total variance in the model output. Traditionally, the FAST assumes model parameter independence. Recently, the dependence between model parameters can be taken into consideration by reordering the sampled parameter values to a specified correlation structure (Xu & Gertner, 2007). The traditional FAST may also have limitations due to the aliasing effect among parameters by using integer characteristic frequencies (i.e. the variance at a specific frequency may be jointly contributed by two or more parameters) (Tarantola *et al*., 2006). The aliasing effect can be overcome by using a random balance design in an improved FAST, which assigns a common characteristic frequency to all the parameters. For more details about the improved FAST, refer to Xu & Gertner (2008).

In our study, the uncertainties are from profile inputs (monthly time series) of different climate variables. In order to use FAST, we need to sample from the ensemble of the 27 climate prediction profiles (CO_2, temperature, precipitation, PAR; see Fig. 3). We also need to consider the dependence of the profiles among different climate variables, because they are commonly correlated (e.g. high temperature profiles are generally associated with the high CO_2 profiles). because the spread/difference of climate variable values across different prediction profiles increased through time (Fig. 3), compared with the earlier prediction values before 2090 AD, the 2090–2099 AD mean climate variable values may best capture the dependence structure of profiles among different climate variables (if there is not enough spread, the calculated correlation structure may be too sensitive to the random error in the prediction data). Thus, in this study, we use the mean of climate variables during the period 2090–2099 AD (for notation convenience, we term them the control variables) as variables to control the sampling of profiles from the ensemble of 27 climate prediction profiles. Namely, we first generate the FAST sample for the control variables (which are scalar variables) and then use the sampled values of the control variable to obtain the sampled profile. In this way, we are able to link the uncertainty in the control variables through the prediction-profile ensemble to the model output. Finally, the FAST analysis can be

Table 2 Global climate model predictions used in the uncertainty and sensitivity analysis

Emission scenarios	Model	Institute	Project
B1	AGCM + OGCM	Center for Climate System Research, National Institute for Environmental Studies, Japan	IPCC TAR
	Mk2.0	Australia's Commonwealth Scientific and Industrial Research Organization, Australia	IPCC TAR
	Mk3.0	Australia's Commonwealth Scientific and Industrial Research Organization, Australia	IPCC FAR
	AOM	Goddard Institute for Space Studies, USA	IPCC FAR
	CM3.0	Institute for Numerical Mathematics, Russia	IPCC FAR
A1T	AGCM + OGCM	Center for Climate System Research, National Institute for Environmental Studies, Japan	IPCC TAR
B2	CGCM2	Canadian Center for Climate Modeling and Analysis, Canada	IPCC TAR
	AGCM + OGCM	Center for Climate System Research, National Institute for Environmental Studies, Japan	IPCC TAR
	Mk2.0	Australia's Commonwealth Scientific and Industrial Research Organization, Australia	IPCC TAR
	HADCM3	Hadley Centre for Climate Prediction and Research, UK	IPCC TAR
	NCAR-PCM	National Centre for Atmospheric Research, USA	IPCC TAR
IS92a	CGCM2	Canadian Center for Climate Modelling and Analysis, Canada	VEMAP
	HADCM3	Hadley Centre for Climate Prediction and Research, UK	VEMAP
A1	AGCM + OGCM	Center for Climate System Research, National Institute for Environmental Studies, Japan	IPCC TAR
	Mk2.0	Australia's Commonwealth Scientific and Industrial Research Organization, Australia	IPCC TAR
A1B	AOM	Goddard Institute for Space Studies, USA	IPCC FAR
	CM3.0	Institute for Numerical Mathematics, Russia	IPCC FAR
	NCAR-PCM	National Centre for Atmospheric Research, USA	IPCC TAR
A2	CGCM2	Canadian Center for Climate Modelling and Analysis, Canada	IPCC TAR
	AGCM + OGCM	Center for Climate System Research, National Institute for Environmental Studies, Japan	IPCC TAR
	Mk2.0	Australia's Commonwealth Scientific and Industrial Research Organization, Australia	IPCC TAR
	Mk3.0	Australia's Commonwealth Scientific and Industrial Research Organization, Australia	IPCC FAR
	HADCM3	Hadley Centre for Climate Prediction and Research, UK	IPCC TAR
	NCAR-PCM	National Centre for Atmospheric Research, USA	IPCC TAR
A1FI	AGCM + OGCM	Center for Climate System Research, National Institute for Environmental Studies, Japan	IPCC TAR

There were three runs for the HADCM3 model under A2 emission scenario in TAR.
IPCC TAR, IPCC Third Assessment Report; IPCC FAR, IPCC Fourth Assessment Report; VEMAP, Vegetation-Ecosystem Modeling and Analysis Project.

conducted on the model with the control variables treated as new model parameters.

Specifically, we first generated a FAST sample for the control variables (i.e. mean of the temperature, precipitation, CO_2 and PAR during the period 2090–2099 AD) based on the correlation structure (Table 3) and the lower and upper boundary for each variable (3.97 and 12.59 °C for temperature, 522.94 and 633.86 μmol $m^{-2} s^{-1}$ for PAR, 79.20 and 105.42 cm for precipitation, and 546.80 and 923.25 ppm for CO_2) using a uniform distribution. The correlation structure of control variables from the 27 climate prediction profiles indicates that the control variable of temperature was significantly correlated with the control variables of PAR and CO_2 (Table 3), although there was no clear correlation among control variables for precipitation, PAR and CO_2. We use a relatively small sample size of 209 for FAST (but this is still adequate for a model with only four parameters), because it takes about 1 h for each simulation. For a specific FAST sample value of a control variable (x_i), we sampled the corresponding monthly values using the nearest neighbor profiles (determined by the control variable values) in

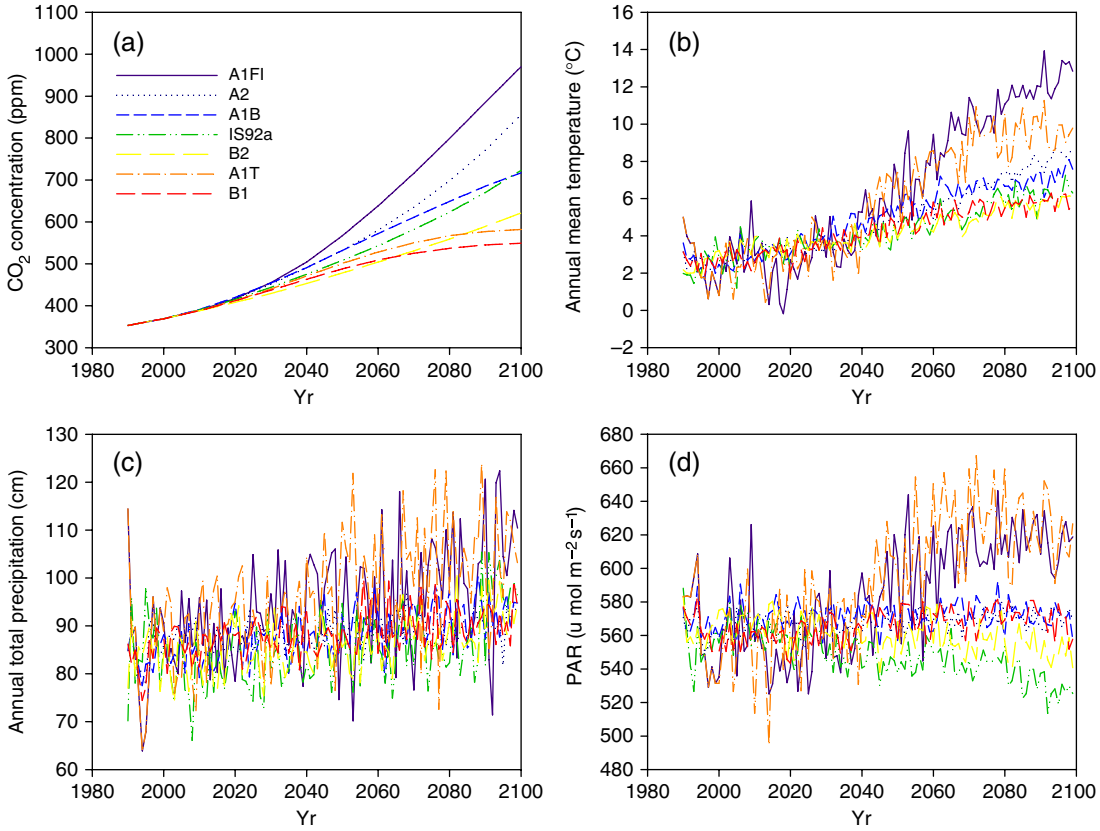

Fig. 3 Mean climate variable change for 27 predictions with seven CO_2 emission scenarios: (a) annual mean CO_2 concentration (ppm); (b) annual mean temperatures (°C); (c) annual precipitation (cm) and (d) annual mean PAR ($\mu mol\, m^{-2}\, s^{-1}$).

Table 3 Spearman rank correlation coefficients of mean climate variables during the period 2090–2099 AD based on 27 global climate model predictions

	Temperature	PAR	Precipitation	CO_2
Temperature	1.00	0.70 (<0.0001)	0.24 (0.23)	0.41 (0.03)
PAR	0.70 (<0.0001)	1.00	0.27 (0.18)	0.07 (0.73)
Precipitation	0.24 (0.23)	0.27 (0.18)	1.00	0.05 (0.79)
CO_2	0.41 (0.03)	0.07 (0.73)	0.05(0.79)	1.00

Values in parentheses indicate the *P*-values of correlation coefficient.
PAR, photosynthetic active radiation.

the ensemble of 27 climate prediction profiles (Table 2). Namely, if there was a prediction profile with the control variable value equal to x_i, then the sampled monthly values of the corresponding climate variable were assigned with the monthly values from the prediction profile. Otherwise, we first located two neighbor prediction profiles which had control variable values next to the sampled value x_i (for example, see Fig. 4a). The sampled monthly climate variable value was assigned based on the inverse distance weighed average of the monthly values from the two neighbor prediction profiles, where the distance weights were calculated based on the difference of x_i from control variable values in the two neighbor prediction profiles.

The nearest neighbor profile sampling method described above can sample the uncertainty through all the months from 2000 to 2099 AD, because the 27 prediction profiles formed reasonable uncertainty bounds through time (Fig. 3). In addition, because the sampled profile tracks the trend of the neighbor profiles, the sampled profile can also capture the autocorrelation in the neighbor profiles from the ensemble

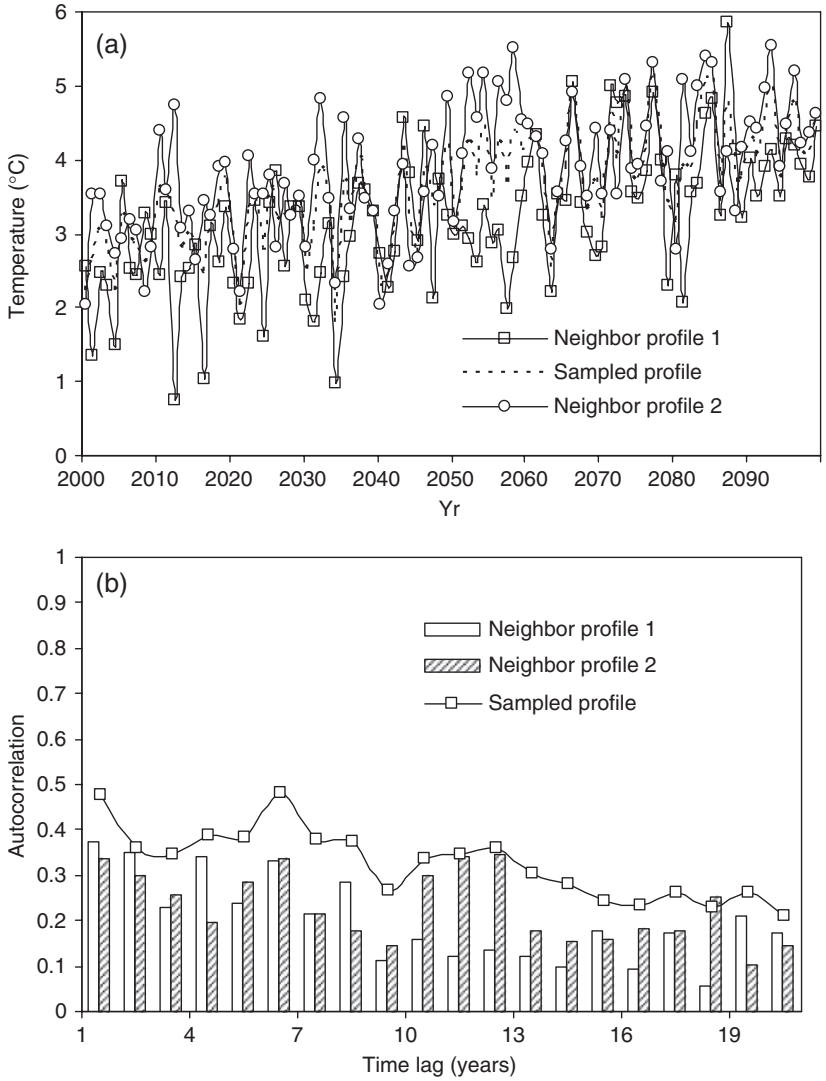

Fig. 4 An example of nearest neighbor profiles sampling (a) and the corresponding autocorrelation (b) for the annual mean temperature. Neighbor profiles 1 and 2 are predicted by models Ck3.1 and AOM under emission scenario B1 (Table 2), with annual mean temperature of 3.97 and 4.61 °C during 2090–2099 AD. The sampled profile has an annual mean temperature of 4.37 °C during 2090–2099 AD.

(Fig. 4b). The correlation structure in Table 3 was used to control the dependence of prediction profiles among different climate variables. For the monthly values in the sampled profiles, due to the variability of monthly values through time, the dependence structure among climate variables may change through time. However, the Spearman rank correlation for the sampled profiles is close to that for the 27 climate prediction ensemble after year 2050 AD (Fig. 5). This suggests that the nearest neighbor profile sampling method can capture the correlation structure in the ensemble when the spread/difference of climate variable values across different prediction profiles is relatively large (Fig. 3). Before year 2050 AD, the correlation structure difference between the sampled profiles and the ensemble is relatively large, because the correlation structure for the earlier prediction values is more sensitive to the random error when the spread/difference of climate variable values across different prediction profiles is relatively small.

A uniform distribution for the climate control variables was assumed, although the sampled distributions from the 27 reference prediction profiles may not be uniformly distributed. However, it would be misleading to use the empirical sampled distribution from 27 reference prediction profiles, because the predictions are not true samples from the future, but are instead based on a subjective selection of scenarios. Without

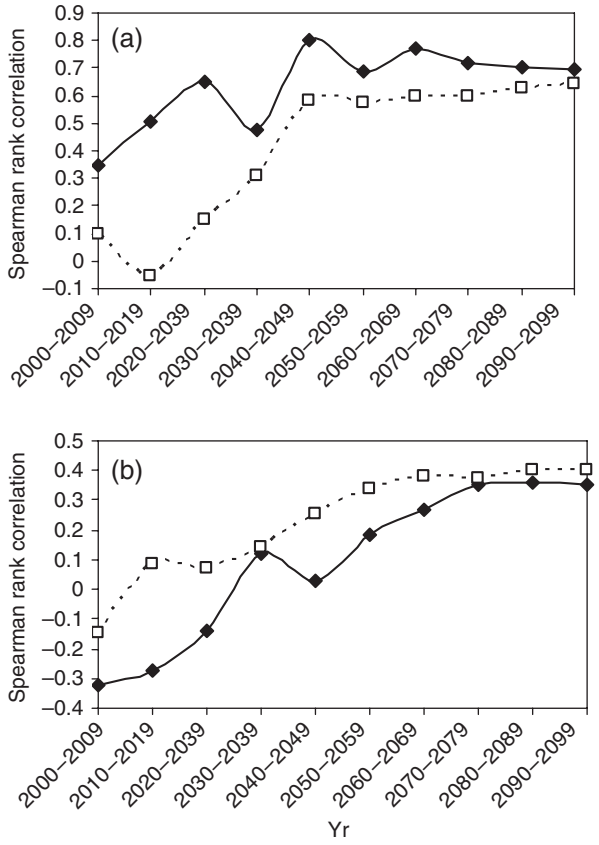

Fig. 5 Comparisons of Spearman rank correlation for the ensemble of 27 climate predictions (the solid line) and the 209 sampled prediction profiles from the ensemble (the dotted line) using the nearest neighbor profiles interpolation: (a) the correlation between PAR and CO_2 and (b) the correlation between temperature and CO_2.

further information about the uncertainty distribution, the uniform distribution is a commonly used conservative choice for uncertainty analysis (Xiu & Sherwin, 2007).

We assumed the climate stabilizes after year 2099 AD. Because most greenhouse gas emission scenarios predict that CO_2 will continue to rise after 2099 AD (IPCC, 2001), our predictions after 2099 AD are conservative. However, this trend of rising CO_2 would not affect the basic results of the uncertainty in forest landscape response and the corresponding uncertainty contributions by different climate variables.

Because of the photorespiration inhibition effect of CO_2, the optimum temperature for photosynthesis of C_3 plants could increase by 5 °C under a doubling of CO_2 (Long, 1991). Xu *et al*. (2007) concluded that an optimum temperature increase induced by CO_2 enrichment may be very important for predicting forest landscape response to climatic change. In this study, we conducted uncertainty and sensitivity analysis for two optimum temperature increase scenarios. The two optimum temperature increase scenarios are (1) there is no optimum temperature increase, and (2) there is a gradual optimum temperature increase by 5 °C over the period 2000–2099 AD (5 °C after year 2099 AD).

An automatic program was built as part of the current study to couple PnET-II model with LANDIS-II model. For each sample element (five sampled profiles of monthly minimum and maximum temperature, precipitation, CO_2 and PAR), a corresponding 2000–2400 AD period forest landscape change was simulated. For LANDIS-II output, we classified the forest into five forest types: aspen–birch (aspen, paper birch and balsam poplar), maple–ash (red maple, sugar maple and white ash), pine (red pine, white pine and jack pine), spruce–fir (white spruce, black spruce and balsam fir) and cedar (white cedar). For a particular landscape cell, the assignment of forest type is based on the cumulative biomass of the five forest types. We used the landscape metric analysis software, APACK (Mladenoff & DeZonia, 2000), to calculate the percentage area of different forest types in the forested ecoregions.

Results

The uncertainty in the forest landscape response to climatic change became very high after 2200 AD (Figs 6 and 7), which is close to the time when many species reach the end of their life span (Table 1). This is because a species can only gain competitive advantage under climatic change when the original forest stands are removed by death or disturbances, except for very shade-tolerant species (e.g. sugar maple) which could quickly gain a competitive advantage in the understory. In this study, we only simulated minor disturbances of windthrow, so the uncertainty in forest landscape response to climatic change will mainly arise after the species reach their longevity. The competitive advantage in the understory for very shade-tolerant species as seedlings may not be reflected in our simulation results, because the assignment of forest type is based on the cumulative biomass. The results also show that the uncertainty in percentage area prediction is much higher for spruce–fir and pine forest types than for other forest types in both scenarios (with and without optimum temperature increase) (Figs 6 and 7). This suggests that the BWCA forest response to climatic change is mainly determined by the relative dominance of spruce–fir and pine forests.

For the sensitivity analysis results for both scenarios (with and without optimum temperature increase), the most important source of uncertainty in forest-type

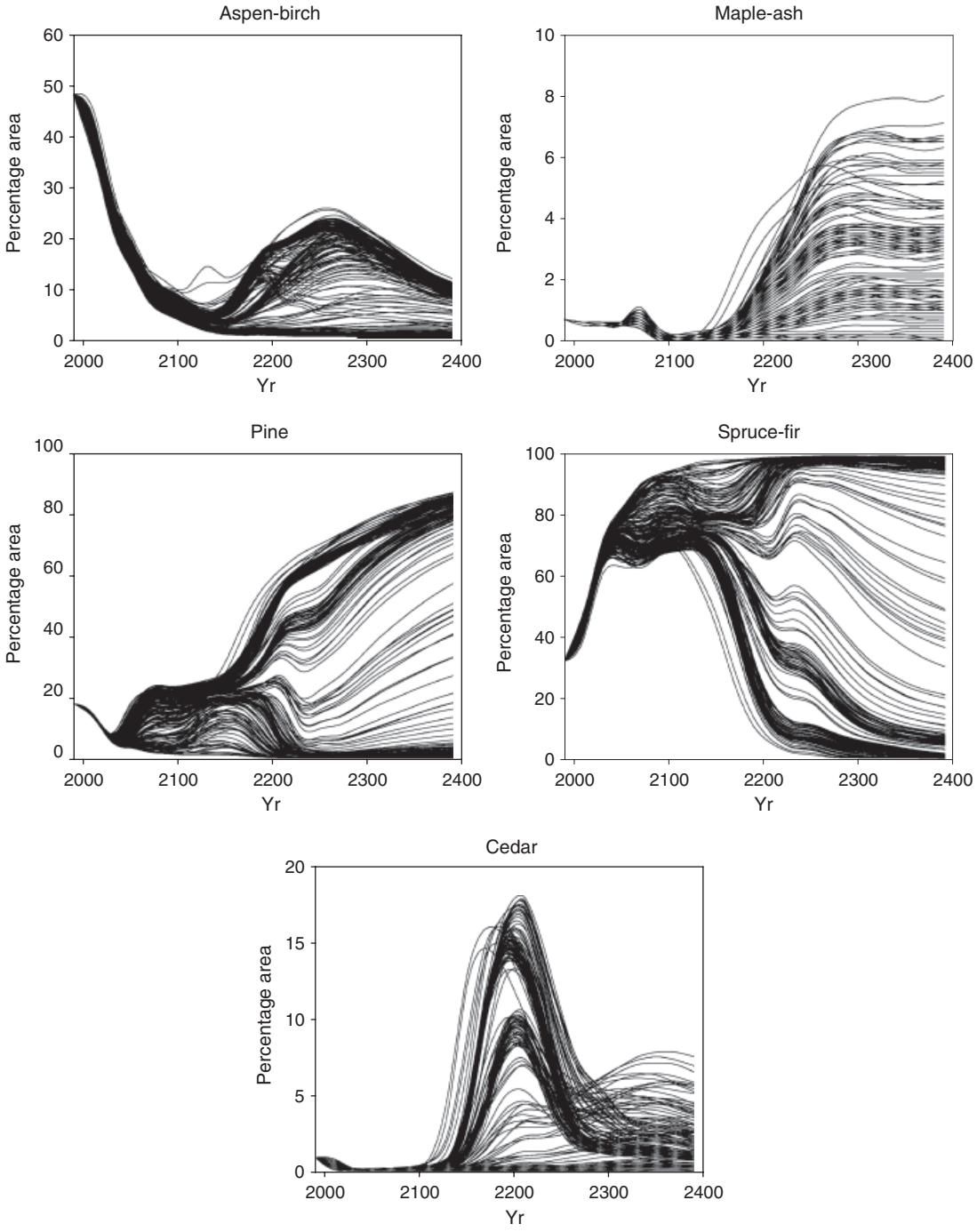

Fig. 6 Uncertainty in forest-type percentage area predictions for the scenario without optimum temperature increase.

composition comes from the uncertainty in temperature prediction (Fig. 8; we did not plot the sensitivity analysis results for the scenario with 5 °C optimum temperature increase, because it has a similar pattern as the scenario without optimum temperature increase). The second most important is PAR, the third is CO_2 and the least important is precipitation.

Because of fire suppression, the BWCA area will likely transition toward spruce–fir-dominated boreal forest under the scenario of continuing the historic 1984–1993 mean climate (Scheller *et al.*, 2005; Xu *et al.*, 2007). Under the predicted climatic change without optimum photosynthetic temperature increase, our results show that the BWCA forest will remain as

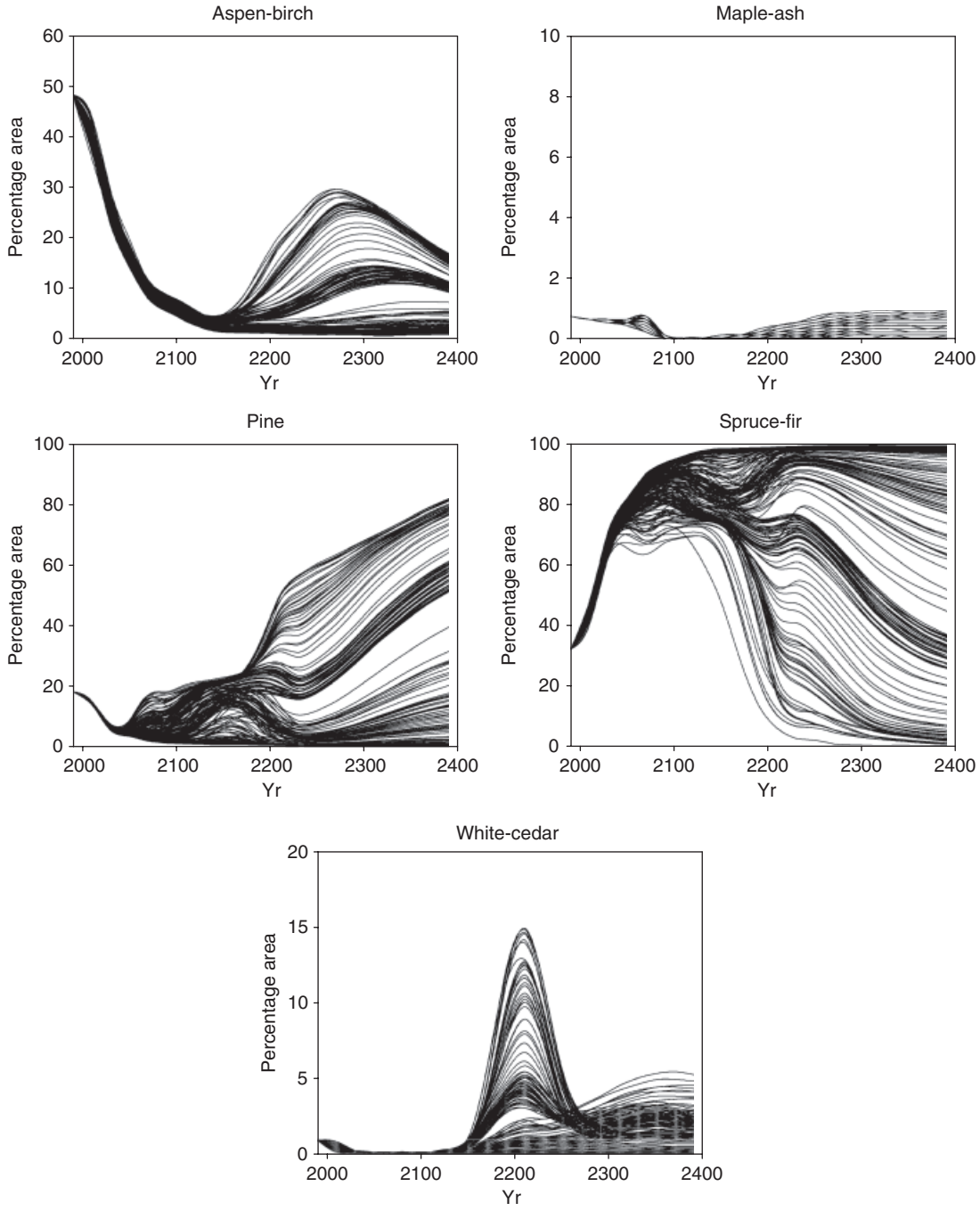

Fig. 7 Uncertainty in forest-type percentage area predictions for the scenario with a gradual optimum temperature increase of 5 °C over the period 2000–2099 AD.

spruce–fir-dominated boreal forest in only 44% of the 209 simulations, while the remaining forests will be pine-dominated mixed forest (Fig. 9). However, if there is a 5 °C gradual increase in optimum photosynthetic temperature over the period 2000–2099 AD, the BWCA forest will remain as spruce–fir-dominated boreal forest in 73% of the 209 simulations. This suggests that the optimum photosynthetic temperature increase induced by the CO_2 enrichment can substantially reduce the forest landscape response to climatic change. Furthermore, percentage area prediction distribution for the 209 simulations is also different under the two scenarios (with and without optimum temperature increase) (Figs 6 and 7). For all forest types except for

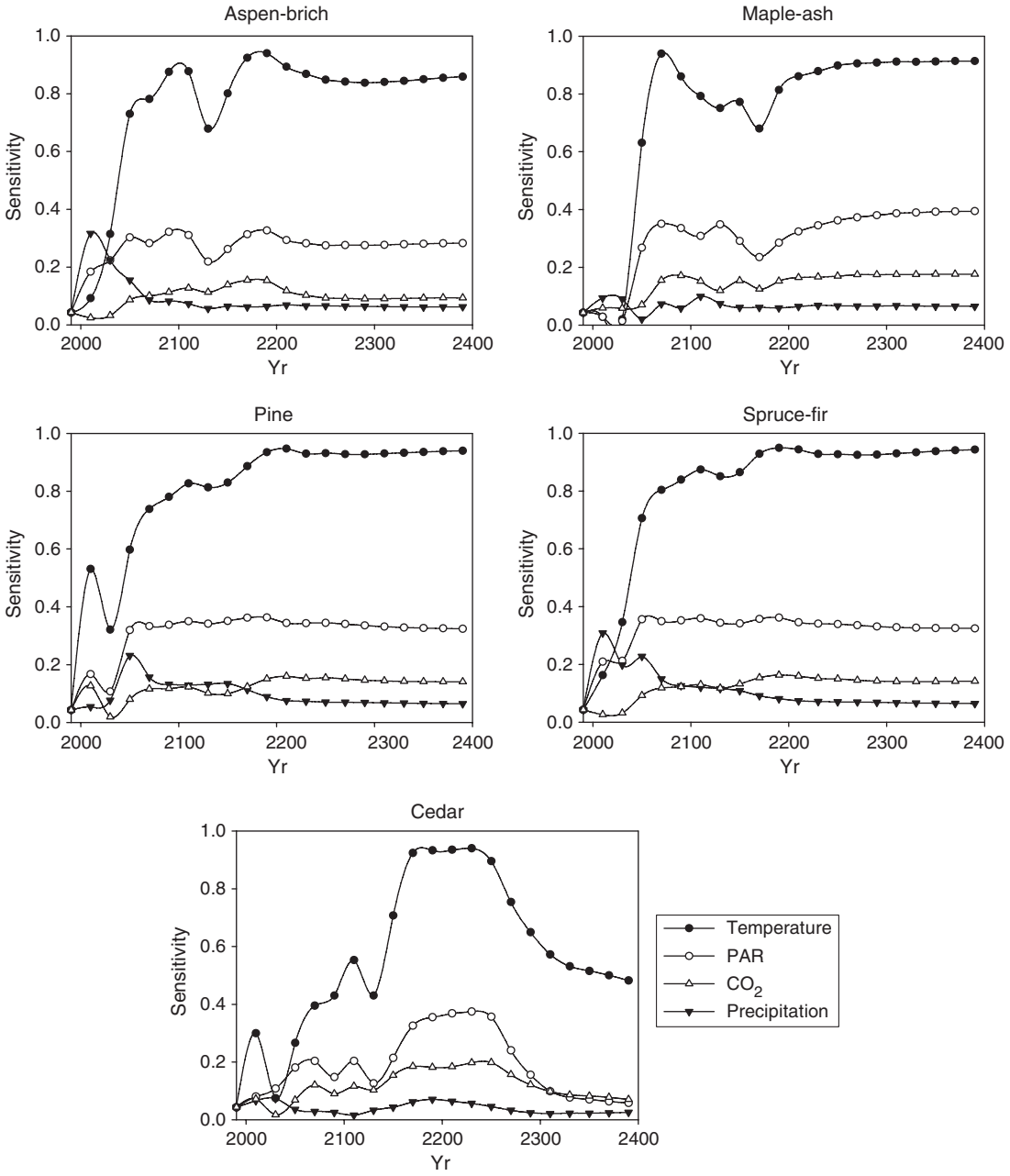

Fig. 8 Sensitivity of forest-type percentage area predictions to sources of uncertainty (temperature, PAR, precipitation and CO_2) for the scenario without optimum temperature increase. The sensitivity is calculated as the ratio of amount of variance contributed by a specific climate variable to the total variance in the model output of forest-type percentages.

spruce–fir, compared with the scenario with a 5 °C optimum temperature increase over the period 2000–2099 AD, there is larger number of simulations with relatively high percentage area under the scenario with no optimum temperature increase. This suggests that there is an increased probability of a more diverse forest landscape under climatic change without optimum temperature increase.

Discussion

Our results show that the uncertainty in the forest landscape response to climatic change becomes very high after 2200 AD. In our study, we assume that the fire suppression practice applied currently will also be successfully applied in the future. However, the future climatic change may increase the fire risk (Westerling

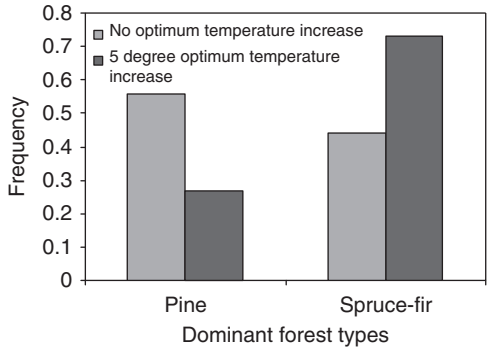

Fig. 9 Predicted dominant forest-type frequencies during the period 2300–2400 AD.

et al., 2006) and the current level of fire suppression may be difficult to maintain. Thus, the forest landscape may have responded earlier and the uncertainty may become high before 2200 AD.

Our results show that precipitation has the lowest uncertainty contribution for simulated BWCA response to climatic change. This is because the precipitation in the BWCA is ample for forest growth, given the cold temperatures and short growing season (Baker, 1989). In addition, the stomatal conductance reduction by CO_2 enrichment may increase the water use efficiency, particularly for deciduous species. This conclusion may not be applicable to other ecosystems. For example, a forest ecosystem in the Eastern Mediterranean region may experience drought under IPCC predictions (Koerner *et al*., 2005), in which case, precipitation may have a high uncertainty contribution. PAR is a very important source of uncertainty in our simulated forest landscape response to climatic change. This is because there is relatively high uncertainty in global climatic change model prediction and PAR is the basic energy input for photosynthesis. CO_2 contributes less than 20% of the uncertainty in forest-type composition prediction. This is because we only measured the direct effect of CO_2 enrichment on photosynthesis and stomatal conductance. The overall contribution of CO_2 to uncertainty in forest-type composition should be much higher than that shown in Fig. 8, because CO_2 is the major greenhouse gas causing the global climatic change. In addition, the forest landscape change in this study is resultant from the interaction among 13 tree species' responses to climatic change. Even if the direct effect of CO_2 is high for individual trees, the contribution to the uncertainty in forest-type composition may be low because the CO_2 effect on photosynthesis may not vary substantially among all species, which is mainly determined by the foliar N content. Compared with CO_2, the temperature contribution should be high because its effect on southern and northern species in the study area is much different, which can result in a very different forest landscape.

The forest landscape response to climatic change is a multiscale complex process. It is very difficult to accurately predict the future response. The modeling predictions generally rely on different assumptions. One major assumption in the uncertainty and sensitivity analysis of forest landscape response to climatic change is that the effect of climatic change on species performance is mainly through the modification of the species establishment probability and ANPP determined by the vegetative growth processes. However, other developmental processes (such as pollen and seed production, early seedling establishment, flowering and mortality) may also be affected (Greenwood *et al*., 2002; Memmott *et al*., 2007). Another important assumption is that we assume there is no feedback of forest composition change to the climate. However, the forest composition can change microclimate which can be important in terms of forest diversity (Dale *et al*., 2001).

Acknowledgements

US Department of Agriculture McIntire-Stennis funds (MS 875-359) and US Army Corps of Engineers Construction Engineering Research Laboratory funds (CERL W9132T-06-2-0001) were used to support this study. We are grateful to two anonymous reviewers for their very detailed comments, which greatly improved this paper.

References

Aber JD, Federer CA (1992) A generalized, lumped-parameter model of photosynthesis, evapotranspiration and net primary production in temperate and boreal forest ecosystems. *Oecologia*, **92**, 463–474.

Aber JD, Ollinger SV, Federer CA *et al*. (1995) Predicting the effects of climate change on water yield and forest production in the Northeastern U.S. *Climate Research*, **5**, 207–222.

Baker WL (1989) Landscape ecology and nature reserve design in the Boundary Waters Canoe Area, Minnesota. *Ecology*, **70**, 23–35.

Baker WL (1992) Effects of settlement and fire suppression on landscape structure. *Ecology*, **73**, 1879–1887.

Botkin DB, Janak JF, Wallis JR (1972) Some ecological consequences of a computer model of forest growth. *Journal of Ecology*, **60**, 849–873.

Castro J, Zamora R, Hodar JA, Gomez JM (2004) Seedling establishment of a boreal tree species (*Pinus sylvestris*) at its southernmost distribution limit: consequences of being in a marginal Mediterranean habitat. *Journal of Ecology*, **92**, 266–277.

Cramer W, Bondeau A, Woodward FI *et al*. (2001) Global response of terrestrial ecosystem structure and function to CO_2 and climate change: results from six dynamic global vegetation models. *Global Change Biology*, **7**, 357–373.

Crosetto M, Tarantola S (2001) Uncertainty and sensitivity analysis: tools for GIS-based model implementation. *International Journal of Geographical Information Science*, **15**, 415–437.

Cukier RI, Levine HB, Shuler KE (1978) Nonlinear sensitivity analysis of multiparameter model systems. *Journal of Computational Physics*, **26**, 1–42.

Dale VH, Joyce LA, McNulty S *et al.* (2001) Climate change and forest disturbances. *Bioscience*, **51**, 723–734.

Drake BG, GonzalezMeler MA, Long SP (1997) More efficient plants: a consequence of rising atmospheric CO_2? *Annual Review of Plant Physiology and Plant Molecular Biology*, **48**, 609–639.

Flannigan MD, Woodward FI (1994) Red pine abundance – current climatic control and responses to future warming. *Canadian Journal of Forest Research*, **24**, 1166–1175.

Frelich LE, Reich PB (1995) Spatial patterns and succession in a Minnesota southern-boreal forest. *Ecological Monographs*, **65**, 325–346.

Greenwood MS, Livingston WH, Day ME, Kenaley SC, White AS, Brissette JC (2002) Contrasting modes of survival by jack and pitch pine at a common range limit. *Canadian Journal of Forest Research*, **32**, 1662–1674.

Hansen AJ, Neilson RR, Dale VH *et al.* (2001) Global change in forests: responses of species, communities, and biomes. *Bioscience*, **51**, 765–779.

He HS, Hao ZQ, Mladenoff DJ, Shao GF, Hu YM, Chang Y (2005) Simulating forest ecosystem response to climate warming incorporating spatial effects in north-eastern China. *Journal of Biogeography*, **32**, 2043–2056.

He HS, Mladenoff DJ, Crow TR (1999) Linking an ecosystem model and a landscape model to study forest species response to climate warming. *Ecological Modelling*, **112**, 213–233.

He HS, Mladenoff DJ, Gustafson EJ (2002) Study of landscape change under forest harvesting and climate warming-induced fire disturbance. *Forest Ecology and Management*, **155**, 257–270.

Heinselman M (1973) Fire in the virgin forests of the Boundary Waters Canoe Area, Minnesota. *Quaternary Research*, **3**, 329–382.

IPCC (2001) *Climate Change 2001: The Scientific Basis*. Cambridge University Press, Cambridge.

Iverson LR, Prasad AM (1998) Predicting abundance of 80 tree species following climate change in the eastern United States. *Ecological Monographs*, **68**, 465–485.

Iverson LR, Prasad AM (2002) Potential redistribution of tree species habitat under five climate change scenarios in the eastern US. *Forest Ecology and Management*, **155**, 205–222.

Iverson LR, Schwartz MW, Prasad AM (2004) Potential colonization of newly available tree-species habitat under climate change: an analysis for five eastern US species. *Landscape Ecology*, **19**, 787–799.

Keane RE, Austin M, Field C *et al.* (2001) Tree mortality in gap models: application to climate change. *Climatic Change*, **51**, 509–540.

Kerr RA (2001) Rising global temperature, rising uncertainty. *Science*, **292**, 192–194.

Kittel TGF, Rosenbloom NA, Kaufman C *et al.* (2000) *VEMAP Phase 2 Historical and Future Scenario Climate Database*. Oak Ridge National Laboratory Distributed Active Archive Center, Oak Ridge, TN, USA.

Koerner C, Sarris D, Christodoulakis D (2005) Long-term increase in climatic dryness in the East-Mediterranean as evidenced for the island of Samos. *Regional Environmental Change*, **5**, 27–36.

Korner C (2006) Plant CO_2 responses: an issue of definition, time and resource supply. *New Phytologist*, **172**, 393–411.

Leggett J, Pepper WJ, Swart RJ *et al.* (1992) Emissions scenarios for the IPCC: an update. In: *Climate Change 1992: The Supplementary Report to the IPCC Scientific Assessment* (eds Houghton JT, Callander BA, Varney SK), pp. 68–95. Cambridge University Press, Cambridge, UK.

Long SP (1991) Modification of the response of photosynthetic productivity to rising temperature by atmospheric CO_2 concentrations – has its importance been underestimated. *Plant, Cell and Environment*, **14**, 729–739.

Long SP, Ainsworth EA, Rogers A, Ort DR (2004) Rising atmospheric carbon dioxide: plants face the future. *Annual Review of Plant Biology*, **55**, 591–628.

Mahlman JD (1997) Uncertainties in projections of human-caused climate warming. *Science*, **278**, 1416–1417.

Medlyn BE, Barton CVM, Broadmeadow MSJ *et al.* (2001) Stomatal conductance of forest species after long-term exposure to elevated CO_2 concentration: a synthesis. *New Phytologist*, **149**, 247–264.

Memmott J, Craze PG, Waser NM, Price MV (2007) Global warming and the disruption of plant–pollinator interactions. *Ecology Letters*, **10**, 710–717.

Mladenoff DJ, DeZonia B (2000) *APACK 2.14 Users Guide*. Department of Forest Ecology and Management, University of Wisconsin-Madison, WI, USA.

Moser WK, Hansen MH, Nelson MD *et al.* (2007) *After the Blowdown: A Resource Assessment of the Boundary Waters Canoe Area Wilderness, 1999–2003*. Northern Research Station, US Department of Agriculture – Forest Service, Newtown Square, PA.

Nakicenovic N, Swart R (2000) *Special Report on Emissions Scenarios: A Special Report of Working Group III of the Intergovernmental Panel on Climate Change*. Cambridge University Press, Cambridge, UK.

Ollinger SV, Aber JD, Reich PB, Freuder RJ (2002) Interactive effects of nitrogen deposition, tropospheric ozone, elevated CO_2 and land use history on the carbon dynamics of northern hardwood forests. *Global Change Biology*, **8**, 545–562.

Osborn T, Briffa KR (2006) The spatial extent of 20th-century warmth in the context of the past 1200 years. *Science*, **311**, 841–844.

Pastor J, Post WM (1985) *Development of a Linked Forest Productivity-Soil Process Model*. Report ORNL/TM-9519, National Laboratory, Oak Ridge, TN.

Pastor J, Post WM (1988) Response of northern forests to CO_2-induced climate change. *Nature*, **334**, 55–58.

Saltelli A, Chan K, Scott M (2000) *Sensitivity Analysis*. John Wiley and Sons, West Sussex.

Saxe H, Ellsworth DS, Heath J (1998) Tree and forest functioning in an enriched CO_2 atmosphere. *New Phytologist*, **139**, 395–436.

Scheller RM, Domingo JB, Sturtevant BR, Williams JS, Rudy A, Gustafson EJ, Mladenoff DJ (2007) Design, development, and application of LANDIS-II, a spatial landscape simulation model with flexible temporal and spatial resolution. *Ecological Modelling*, **201**, 409–419.

Scheller RM, Mladenoff DJ (2004) A forest growth and biomass module for a landscape simulation model, LANDIS: design, validation, and application. *Ecological Modelling*, **180**, 211–229.

Scheller RM, Mladenoff DJ (2005) A spatially interactive simulation of climate change, harvesting, wind, and tree species migration and projected changes to forest composition and biomass in northern Wisconsin, USA. *Global Change Biology*, **11**, 307–321.

Scheller RM, Mladenoff DJ, Crow TR, Sickley TA (2005) Simulating the effects of fire reintroduction versus continued fire absence on forest composition and landscape structure in the Boundary Waters Canoe Area, Northern Minnesota, USA. *Ecosystems*, **8**, 396–411.

Schwartz SE, Smith TM, Karl TR, Reynolds RW (2002) Uncertainty in climate models. *Science*, **296**, 2139–2140.

Shafer SL, Bartlein PJ, Thompson RS (2001) Potential changes in the distributions of Western North America tree and shrub taxa under future climate scenarios. *Ecosystems*, **4**, 200–215.

STATSGO (1994) *State Soil Geographic (STATSGO) Data Base*. Report number 1492, US Department of Agriculture National Cartography and GIS Center, Fort Worth, TX.

Suttle KB, Thomsen MA, Power ME (2007) Species interactions reverse grassland responses to changing climate. *Science*, **315**, 640–642.

Sykes MT, Prentice IC (1995) Boreal forest futures – modeling the controls on tree species range limits and transient responses to climate change. *Water, Air and Soil Pollution*, **82**, 415–428.

Tarantola S, Gatelli D, Mara TA (2006) Random balance designs for the estimation of first order global sensitivity indices. *Reliability Engineering and System Safety*, **91**, 717–727.

Thornton PE, Running SW, White MA (1997) Generating surfaces of daily meteorological variables over large regions of complex terrain. *Journal of Hydrology*, **190**, 214–251.

Thuiller W (2004) Patterns and uncertainties of species' range shifts under climate change. *Global Change Biology*, **10**, 2020–2027.

Urban DL, Harmon ME, Halpern CB (1993) Potential response of Pacific northwestern forests to climatic change, effects of stand age and initial composition. *Climatic Change*, **23**, 247–266.

Weaver AJ, Zwiers FW (2000) Uncertainty in climate change. *Nature*, **407**, 571–572.

Westerling AL, Hidalgo HG, Cayan DR, Swetnam TW (2006) Warming and earlier spring increase western U.S. forest wildfire activity. *Science*, **313**, 940–943.

Xiu D, Sherwin SJ (2007) Parametric uncertainty analysis of pulse wave propagation in a model of a human arterial network. *Journal of Computational Physics*, **226**, 1385–1407.

Xu C, Gertner GZ (2007) Extending a global sensitivity analysis technique to models with correlated parameters. *Computational Statistics and Data Analysis*, **51**, 5579–5590.

Xu C, Gertner GZ (2008) A general first-order global sensitivity analysis method. *Reliability Engineering and System Safety*, **93**, 1060–1071.

Xu C, Gertner GZ, Scheller RM (2007) Potential effects of interaction between CO_2 and temperature on forest landscape response to global warming. *Global Change Biology*, **13**, 1469–1483.

Xu C, He HS, Hu Y, Chang Y, Larsen DR, Li X, Bu R (2004) Assessing the effect of cell-level uncertainty on a forest landscape model simulation in northeastern China. *Ecological Modelling*, **180**, 57–72.

